

# Detrimental effect of systemic antimicrobial CD4<sup>+</sup> T-cell reactivity on gut epithelial integrity

Cheong K.C. Kwong Chung,<sup>1</sup>  
Francesca Ronchi<sup>1</sup> and  
Markus B. Geuking<sup>1,2</sup>

<sup>1</sup>Department of Clinical Research (DKF),  
Mucosal Immunology Laboratory, University  
of Bern, Bern, Switzerland and <sup>2</sup>Department  
of Microbiology, Immunology and Infectious  
Diseases, Snyder Institute for Chronic Dis-  
eases, Cumming School of Medicine, Univer-  
sity of Calgary, Calgary, AB, Canada

doi:10.1111/imm.12682

Received 2 August 2016; revised 9 October  
2016; accepted 17 October 2016.

Correspondence: Dr Markus Geuking,  
Department of Microbiology, Immunology  
and Infectious Diseases, Health Sciences  
Centre, Cumming School of Medicine,  
University of Calgary, Room 1885, 3330  
Hospital Drive N.W., Calgary, AB T2N 4N1,  
Canada. Email: markus.geuking@ucalgary.ca  
Senior author: Dr. Markus Geuking

## Introduction

Intestinal colonization with commensal bacteria starts at birth. The highest bacterial densities, up to 10<sup>12</sup> colony-forming units (CFU)/g, are reached in the large intestine.<sup>1</sup> It is well accepted that the intestinal microbiota is beneficial for the host by synthesizing vitamins,<sup>2</sup> digesting resistant starch, producing short-chain fatty acids, completing the bile salt cycle, providing colonization resistance to pathogens, and promoting maturation of the immune system.<sup>3,4</sup> In return, the host provides the commensal bacteria with an excellent niche and a constant supply of nutrients. Functional compartmentalization of the mucosal and systemic immune systems, which limits mucosal

## Summary

Healthy host–microbe mutualism relies on compartmentalization and proper regulation of systemic and mucosal immune responses. Nevertheless, the systemic immune system is frequently exposed to bouts of bacteraemia, which can trigger systemic antimicrobial immune reactivity including CD4<sup>+</sup> T cells. Low-level bacteraemia can occur when immune compartmentalization is compromised, for example in the presence of innate immune deficiency or following use of non-steroidal anti-inflammatory drugs. We generated an *Escherichia coli* strain expressing a defined T helper neo-epitope to study systemic antigen-specific antimicrobial CD4<sup>+</sup> T cells and their potential involvement in the pathogenesis of inflammatory bowel diseases. We found that the dose of bacteria required for the induction of systemic antimicrobial CD4<sup>+</sup> T-cell proliferation was high and not easily reached under physiological conditions. Importantly, however, when intestinal barrier function was compromised by induced damage to the intestinal epithelium, the presence of systemic antimicrobial CD4<sup>+</sup> T cells specific for a single neo-antigen resulted in dramatically increased levels of bacterial translocation. This study therefore demonstrates that systemic antimicrobial CD4<sup>+</sup> T-cell reactivity might impact adversely on the mucosa under conditions of reduced barrier function and that despite strong mucosal immune regulation, antigen-specific recognition is still sensitive.

**Keywords:** antigen specificity; CD4<sup>+</sup> T cells; epithelial integrity; host–microbe mutualism; systemic antimicrobial reactivity.

responses to the mucosa, is an important component in the maintenance of host–microbe mutualism.<sup>5–8</sup> This compartmentalization explains why clean laboratory mice (including specific-pathogen free mice) do not usually display systemic antibody<sup>5</sup> or CD4<sup>+</sup> T-cell responses<sup>8</sup> directed against the microbiota. However, systemic responses can occur when immune compartmentalization is compromised,<sup>7</sup> or as a consequence of innate immune deficiency allowing systemic translocation of intestinal bacteria.<sup>9</sup> Bacteria reaching the blood or the spleen following translocation induce strong adaptive immune responses.<sup>10</sup> Importantly, systemic antimicrobial immune reactivity against bacterial antigens, such as the outer membrane porin C (ompC), can be detected even in

Abbreviations: ASF, altered Schaedler flora; CFSE, carboxyfluorescein succinimidyl; CFU, colony-forming unit; DSS, dextran sodium sulphate; IBD, inflammatory bowel disease; IL, interleukin; IMDM, Iscove's modified Dulbecco's medium; LB, Luria–Bertani; MLN, mesenteric lymph node; ompC, outer membrane porin C

healthy individuals.<sup>11</sup> This is probably because, unlike clean laboratory mice, the human systemic immune system is regularly exposed to low levels of gut-derived bacteria through episodes of reduced intestinal barrier function induced by infections,<sup>12</sup> mucosal damage due to dental hygiene,<sup>13</sup> non-steroidal anti-inflammatory drugs,<sup>14</sup> or dietary fats.<sup>15,16</sup> Systemic bacterial translocation has been demonstrated to induce T helper type 1 cells that have the capacity to form memory T cells.<sup>17</sup>

Although systemic bacteria are usually rapidly cleared by the innate immune system,<sup>18–21</sup> the consequences of induced systemic adaptive antimicrobial (hyper-)reactivity, in particular antimicrobial CD4<sup>+</sup> T-cell reactivity, on host–microbe mutualism at the mucosa remains unclear. In humans, systemic antimicrobial hyper-reactivity has been suggested to be involved in the pathogenesis of inflammatory bowel disease (IBD).<sup>22</sup>

To study systemic antimicrobial CD4<sup>+</sup> T-cell responses, we generated an *Escherichia coli* strain expressing a defined T helper cell neo-epitope introduced into ompC. In combination with adoptive transfer of T-cell receptor transgenic T cells specific for this epitope this allowed us to study systemic antimicrobial *E. coli*-specific CD4<sup>+</sup> T-cell responses and their impact on the mucosa. Our experiments were performed in gnotobiotic mice colonized with an altered Schaedler flora (ASF)<sup>23</sup> because these mice can be colonized with *E. coli* but do display a normal immune status.<sup>24</sup> Specific pathogen-free mice are resistant to *E. coli* colonization and can therefore not be used for this study.<sup>25</sup> We found that although the systemic bacterial load required to trigger systemic antimicrobial CD4<sup>+</sup> T-cell proliferation was relatively high and was not reached under steady-state conditions, dextran sulphate sodium (DSS)-induced damage to the colon epithelial barrier caused a tremendously increased bacterial translocation in the presence of systemic antimicrobial CD4<sup>+</sup> T cells specific for the single added neo-antigen. Importantly, DSS treatment of gnotobiotic ASF does not cause overt intestinal inflammation.<sup>24</sup> These data suggest that under situations of disturbed gut integrity, systemic antimicrobial T-cell reactivity, even to a single epitope, can have adverse effects on mucosal integrity. Elucidating the immunological mechanisms involved will be important to better understand the consequences of systemic antimicrobial CD4<sup>+</sup> T-cell reactivity on host–microbe mutualism and their role in the pathogenesis and chronicity of IBD.

## Materials and methods

### Mice

Germ-free and ASF C57BL/6 and SMARTA mice were housed at the gnotobiotic Clean Mouse Facility of the University of Bern. Germ-free mice were bred in flexible

film isolators at the Clean Mouse Facility and absence of bacterial colonization was verified by plating or liquid cultures of the intestinal contents under aerobic and anaerobic conditions, as well as performing Gram and DNA (Sytox green) staining of caecal contents to detect unculturable bacteria. Specific pathogen-free OT-II mice on a C57BL/6 background were obtained from the Zentrale Tierställe of the Medical Faculty of the University of Bern and from the animal facility at the University of Lausanne. All experiments were performed in accordance with the Swiss Federal and Cantonal animal regulations.

### Generation of *E. coli* ompC\_gp61 by $\lambda$ red recombination

The ompC gene of wild-type *E. coli* MG1655 was first replaced with a TetRA cassette by  $\lambda$  red recombination<sup>26</sup> using an amplified TetRA cassette with 40-bp homologous overhangs in combination with pKD46 (Nature Technology Corporation, Lincoln, Nebraska, USA) to target the ompC locus. Clones with successful targeting of the ompC locus ( $\Delta$ ompC::TetRA) were screened for using tetracycline resistance. The ompC\_gp61 construct with the gp61 sequence inserted into loop 7 of ompC was generated by assembly PCR using a synthetic gp61-coding fragment in combination with PCR amplified 5'- and 3'-coding regions of ompC with additional 500-bp homologous regions to target the ompC locus that had been replaced with a TetRA cassette. Recombination was again performed using the targeting construct in combination with pKD46 (Nature Technology Corporation) and recombined clones ( $\Delta$ ompC::ompC\_gp61) were identified by positive selection for loss of TetRA using fusaric acid.<sup>27</sup> Fifty clones were isolated and sequenced to check for mutations.

### *Escherichia coli* strains, cultures and quantification

Wild-type *E. coli* MG1655 was used as the parental strain to generate the ompC-deficient *E. coli*  $\Delta$ ompC ( $\Delta$ ompC::TetRA) and *E. coli* ompC\_gp61 ( $\Delta$ ompC::ompC\_gp61). *Escherichia coli* deficient in both ompC and ompF (*E. coli*  $\Delta$ ompC $\Delta$ ompF) was a generous gift from Prof. Robin Ghosh.<sup>28</sup> To grow *E. coli*, a single colony was inoculated in fresh Luria–Bertani (LB) medium and grown for 16 hr at 37° with shaking at 160 rpm. Bacteria were collected by centrifugation (4000 g for 10 min at 4°) and the bacterial pellet was washed with sterile PBS. Pellets were re-suspended in sterile PBS and the volume was adjusted to obtain the desired amount of CFU in 500  $\mu$ l for gavage or intravenous injection. To assess the bacterial load in the blood, blood was collected in heparin tubes and 50  $\mu$ l of blood was plated on LB medium. To measure the bacterial load in faecal pellets, spleen, liver, or mesenteric

lymph nodes (MLN), the samples were weighed and put into 1 ml PBS containing 0.1% Tergitol (Sigma, St Louis, Missouri, USA). The samples were disaggregated in a Tissuelyser at 30 Hz for 3 min. Then, 50  $\mu$ l of the tissue suspension was plated on LB medium. *Escherichia coli* and *Lactobacillus* were distinguished based on colony morphology and CFU were counted and normalized to the weight of the organs.

#### *In vitro high osmolarity survival test*

$10^4$  CFU of the different *E. coli* strains were incubated at room temperature in either 1 ml of 0.15 M or 1.5 M NaCl. Fifty microlitres of the bacterial suspension was sampled before and 1–3 hr after incubation and plated.

#### *Cell isolation from the colon lamina propria*

Colons were flushed with Dulbecco's Phosphate-Buffered Saline (DPBS) without  $\text{CaCl}_2$  and  $\text{MgCl}_2$  (Invitrogen, Carlsbad, California, USA) and opened longitudinally. The colon was then cut into 3–5 mm pieces and washed four or five times in 20 ml DPBS containing 0.5 mM EDTA and 10 mM HEPES (Invitrogen) at 37° with shaking at 220 rpm to remove the epithelial cell layer. The solution was then transferred into Iscove's modified Dulbecco's medium (IMDM; Invitrogen) containing 0.5 mg/ml collagenase Type VIII (Sigma) and 50 U DNase I to be digested for 40 min at 37° with shaking at 220 rpm. Undigested colon pieces were disaggregated using an 18G needle (BD Biosciences, San Jose, California, USA) and cell suspension was washed with IMDM at 800 g for 10 min. The cell pellet was resuspended in 10 ml IMDM and poured onto a 30%/100% Percoll gradient (GE Healthcare, Little Chalfont, United Kingdom). Following centrifugation at 680 g for 30 min with the acceleration and brake turned off, cells lying at the 30%–100% interphase were collected and used for FACS staining.

#### *Magnetic cell sorting*

Spleens and MLN were digested with 1 U/ml liberase for 30 min at 37° and disintegrated to obtain single cell suspensions. Following centrifugation at 450 g for 5 min, the cell pellet was re-suspended in 1 ml of 0.88%  $\text{NH}_4\text{Cl}$  for 3 min to lyse the red blood cells. Cells were washed in IMDM (Invitrogen) and re-suspended in 300  $\mu$ l of MACS buffer (2% fetal calf serum and 2 mM EDTA in PBS). For  $\text{CD4}^+$  T-cell enrichment 40  $\mu$ l of  $\text{CD4}$  microbeads (Miltenyi Biotec, Bergisch Gladbach, Germany) was added to the cell suspension and incubated for 30 min at 4°. For  $\text{CD11c}^+$  dendritic cell enrichment, 40  $\mu$ l of  $\text{CD11c}$  microbeads (Miltenyi Biotec) was used. After washing in MACS buffer, the cell suspension was filtered through a MACS pre-separation filter (Miltenyi Biotec) and then

added to an MS column (Miltenyi Biotec) on an OctoMACS Separator (Miltenyi Biotec). Positively labelled cells were sorted according to the manufacturer's instructions and purity was assessed by flow cytometry.

#### *CFSE and CellTrace violet labelling*

The MACS-enriched  $\text{CD4}^+$  T cells were re-suspended in PBS at  $1 \times 10^7$  cells/ml. Cells were labelled with 5  $\mu$ M carboxyfluorescein succinimidyl ester (CFSE; Invitrogen) or with 5  $\mu$ M CellTrace violet (Invitrogen) and incubated at 37° for 10 min, followed by the addition of 2% fetal calf serum. After centrifugation for 5 min at 450 g, the supernatant was discarded and the cells were washed in PBS. The cell pellet was re-suspended in PBS at  $6 \times 10^7$  cells/ml and 500  $\mu$ l of CFSE-labelled  $\text{CD4}^+$  T cells were injected into the tail vein.

#### *Preparation of crude outer membrane protein fractions*

An overnight culture of the *E. coli* strain of interest was diluted 100-fold in 500 ml fresh LB medium. The bacteria were grown to an optical density 0.5 (measured at 600 nm) and were harvested by centrifugation at 3500 g for 10 min. The bacteria pellet was resuspended in 5 ml of 20 mM sodium phosphate buffer (pH 7.1) and the bacteria were lysed by sonication (six cycles, one cycle: 30 seconds sonication and 30 seconds cooling on ice). The lysed bacteria were then incubated at room temperature for 35 min in 0.5% sodium *N*-lauryl sarcosinate (Sigma). Following centrifugation at 3000 g for 1 min, the supernatant was collected. Outer membrane protein fraction was enriched in *ompC* by ultracentrifugation at 393 000 g for 14 min. The pellet containing *ompC*-enriched outer membrane protein was resuspended in 20 mM PBS containing 1% sodium dodecyl sulphate.

#### *In vitro proliferation assay*

$\text{CD4}^+$  T cells and dendritic cells were isolated from the spleen and lymph nodes by MACS enrichment. Then,  $2 \times 10^5$  CFSE-labelled  $\text{CD4}^+$  T cells and  $5 \times 10^4$  DC were added to individual wells of round-bottom plates (Sarstedt, Newton, North Carolina, USA) and incubated with 1  $\mu$ g/ml of  $\alpha\text{CD3}$ , 2 ng of gp61 peptide, or 1–100  $\mu$ g/ml of outer membrane proteins that are enriched in *ompC*.  $\text{CD4}^+$  T-cell proliferation was assessed after 5 days of culture using CFSE dilution as a marker of proliferation.

#### *Flow cytometry*

Cells were washed twice with PBS and then stained with an eFluor506 fixable viability dye (eBioscience, San Diego, California, USA) in PBS for 30 min at 4°. Cells were then

washed with FACS buffer containing 2% fetal calf serum (Invitrogen), 2.5 mM EDTA (MP Biomedicals, Santa Ana, California, USA) and 0.1% NaN<sub>3</sub> (Sigma) in PBS. For cell surface marker staining, the cell pellet was re-suspended in 100 µl of antibodies diluted in FACS buffer and stained for 15 min at 4°. The following monoclonal antibodies were used: CD4-PacificBlue clone RM4-5 (Biolegend, San Diego, California, USA), CD90.2-AlexaFluor700 clone 30-H12 (Biolegend), Vα2-Biotin clone B20.1 (BD Biosciences) in combination with Streptavidin-allophycocyanin (APC) (BD Biosciences), CD3-AlexaFluor700 clone 17A2 (Biolegend), CD25-Peridinin chlorophyll protein-Cy5.5 clone PC-61 (Biolegend), CD44-APC-Cy7 clone Im7, CD27-APC clone LG.3A10 (Biolegend), Foxp3-AlexaFluor700 clone FJK-16s (eBioscience), CD19-AlexaFluor700 clone 6D5 (Biolegend), CD11b-APC clone MI/70, CD11c-PE clone HL3 (BD Biosciences) and IA/IE-AlexaFluor700 clone M5/114.15.2 (Biolegend). For intracellular cytokine staining, cells were first stimulated with 50 ng/ml PMA (Sigma) and 750 ng/ml ionomycin (Invitrogen) in the presence of 10 µg/ml Brefeldin-A (Sigma) for 4 hr at 37°. Cells were then washed twice with PBS and the staining with viability dye and cell surface markers was performed as described above. After surface staining, cells were fixed and permeabilized in BD cytofix/cytoperm (BD Biosciences) for 10 min at room temperature in the dark. Following washing with BD wash buffer, cells were stained with following monoclonal antibodies in BD wash buffer overnight: interferon-γ-FITC clone XMG1.2 (BD Biosciences) and interleukin-17 (IL-17) - phycoerythrin clone TC11-18H10 (BD Biosciences). Acquisition was performed on a FACS LSR II SORP (BD Biosciences) and data analysis was performed using FLOWJO software (Tree Star, Ashland, Oregon, USA) and PRISM (GraphPad, La Jolla, San Diego, California, USA). The proliferation index from CFSE dilution profiles was calculated using FLOWJO software (TreeStar).

#### DSS treatment

For DSS (MP Biomedicals) treatment, DSS powder was dissolved in sterile water (Baxter) and sterile filtered. For DSS experiments with SMARTA T-cell transfer, ASF mice were treated with 2% DSS in the drinking water for 9 days. Two days after the start of the DSS treatment, ASF C57BL/6 mice received  $3 \times 10^7$  CFSE-labelled SMARTA T cells followed by gavage or intravenous injection with *E. coli* the following day.

#### Albumin ELISA

Albumin levels in caecal contents were measured using the Mouse albumin ELISA kit (Bethyl Laboratories, Montgomery, Texas, USA). Nunc-Immuno Plates C96 MaxiSorp (Milian, Gahanna, Ohio, USA) were coated

with 50 µl of unlabelled goat anti-mouse albumin antibody (1 : 200 in 0.1 M bicarbonate buffer) overnight at 4°. After washing with 0.05% Tween (Sigma) in PBS and blocking in 1% BSA in PBS, standards (1 mg/ml) and samples (resuspended in PBS) were added to the plate and serial dilutions (1 : 3) were performed. After incubation for 2 hr at room temperature, plates were washed followed by the addition of 50 µl of horseradish peroxidase-conjugated goat anti-mouse albumin antibody (1 in 33 000 in 1% BSA/PBS) for 1 hr at 37°. After washing, the plates were developed using 100 µl of TMB substrate (Biolegend) and stopped using 1M sulphuric acid. The plates were read at 450 nm and analysis was performed with GRAPHPAD PRISM (Graphpad).

#### Cytokine multiplex assay

The cytokines IL-18, IL-6, CXCL1, IP-10/CXCL10, MCP-2/CCL2, MCP-3/CCL7, MIP-1α/CCL3, and RANTES/CCL5 in serum were measured using the ProcartaPlex Mouse Cytokine & Chemokine Panel 1 assay (eBioscience) according to the manufacturer's instructions.

#### Statistics

The unpaired *t*-test was used to assess statistical significance between two groups unless stated otherwise. For non-normally distributed data sets, the non-parametric two-tailed Mann-Whitney test was used. *P*-values below 0.05 were considered significant. GRAPHPAD PRISM software (GraphPad) was used to perform the statistical tests.

## Results

### Generation of a recombinant *E. coli* MG1655 strain expressing the gp61 T helper cell neo-epitope

To study antigen-specific antimicrobial CD4<sup>+</sup> T-cell responses we generated a recombinant *E. coli* MG1655 strain expressing the lymphocytic choriomeningitis virus-derived I-A<sup>b</sup>-restricted T helper cell epitope gp61. This peptide is recognized by T-cell receptor transgenic SMARTA T cells.<sup>29</sup> This epitope was chosen because of the available experimental tools and although it is originally virus-derived, it has now been introduced into a purely bacterial background. The sequence encoding the gp61 epitope was codon optimized for *E. coli* and inserted into loop 7 of the outer membrane porin C (ompC) of *E. coli* MG1655 (Fig. 1a). The chromosomal wild-type ompC gene was replaced with the modified ompC\_gp61 by λ red recombination (see Materials and methods section).<sup>26</sup> This approach was chosen (i) to ensure stable chromosomal integration, rather than plasmid-based expression with the risk of plasmid loss *in vivo*, and (ii) because the integration site in loop 7 of

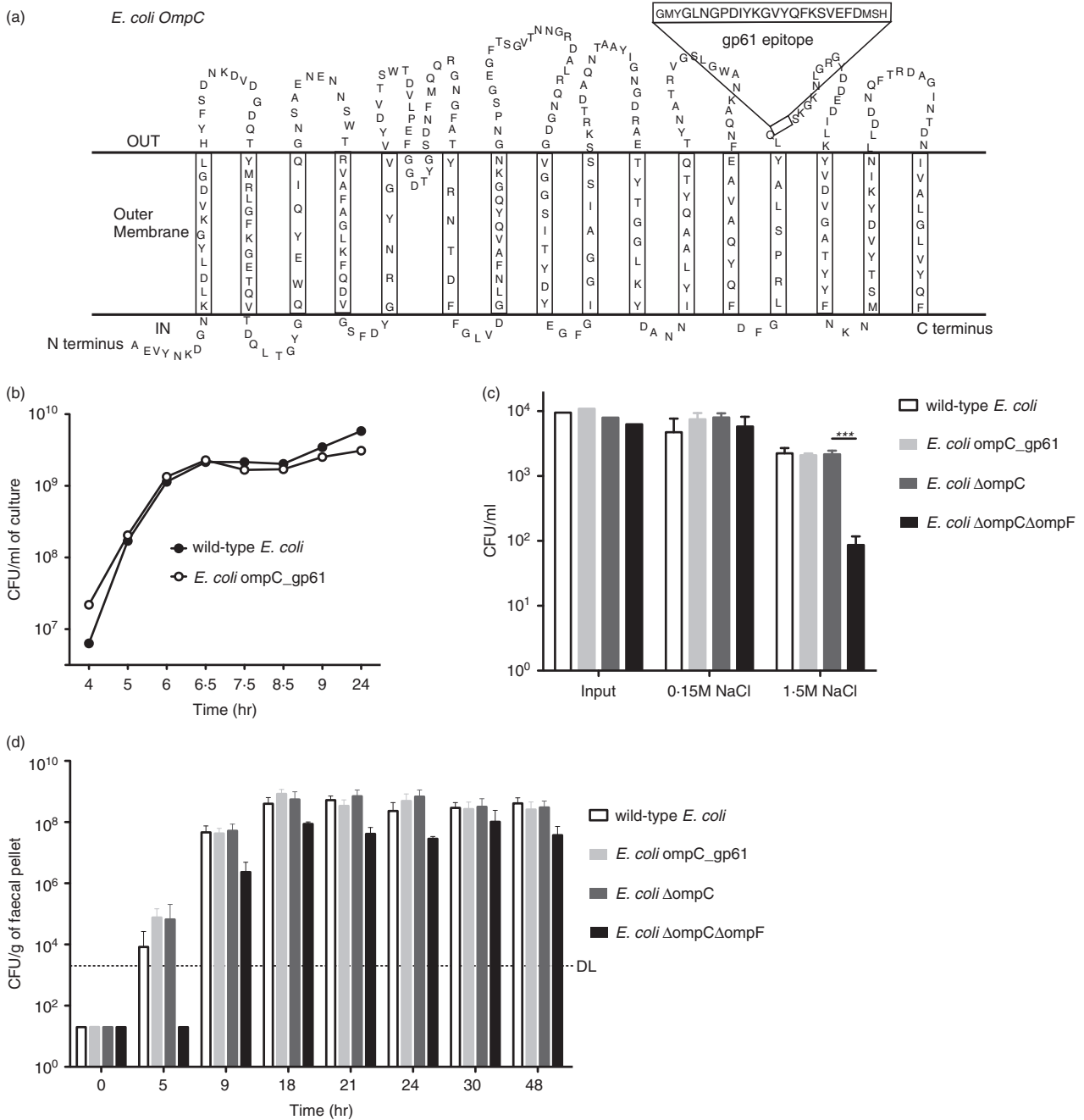


**Figure 1.** *In vitro* characterization of *Escherichia coli* ompC\_gp61. (a) Mutation-free amino acid sequence of ompC after insertion of the gp61 epitope into loop 7. (b) *In vitro* growth curve in Luria-Bertani (LB) medium. Fifty millilitres of LB medium was inoculated with one colony of either wild-type *E. coli* or *E. coli* ompC\_gp61. (c) 10<sup>4</sup> CFU of the indicated *E. coli* strains were treated with 0.15 M or 1.5 M NaCl at room temperature. (d) Germ-free C57BL/6 mice (five mice per group) were gavaged with 10<sup>3</sup> CFU of the indicated *E. coli* strains and colonization levels in faecal pellets were followed. Data shown are representative of two or three independent experiments. Error bars represent mean ± SD. \*\*\**P* < 0.0005.

ompC has previously been shown to be immunogenic and suited for antigen display.<sup>30</sup> Multiple *E. coli* clones that had successfully recombined were isolated and sequenced to check for unwanted mutations introduced during the process. One clone displayed a completely

mutation-free amino acid sequence for the mature ompC and a single mutation (V9N) within the hydrophilic H-region of the signal peptide, which is cleaved off (see Supplementary material, Fig. S1). The cleavage site in the C-region of the signal peptide remained intact. This



*E. coli* strain ( $\Delta ompC::ompC\_gp61$ ) is referred to as *E. coli* ompC\_gp61.

We deliberately generated our own novel antigen-specific antimicrobial T-cell model to be able to perform very precise and well-controlled gnotobiotic experiments. Using this model we can generate basically identical microbiotas that only differ in one single defined epitope coming from one single species (*E. coli*). The T-cell receptor transgenic CBir1 model, which is specific for a flagellin-derived epitope,<sup>31</sup> has two important caveats in this respect. First, flagellin is expressed by a variety of different species, and second, this makes it impossible, even using gnotobiotic technology, to generate a corresponding control microbiota that lacks the flagellin epitope.

We first compared the fitness of the wild-type *E. coli* and the modified *E. coli* ompC\_gp61. Both strains showed identical *in vitro* growth in standard LB broth (Fig. 1b). We next tested the survival of wild-type *E. coli*, *E. coli* ompC\_gp61, *E. coli*  $\Delta ompC$  and *E. coli*  $\Delta ompC\text{-}\Delta ompF$  in high osmolarity conditions (Fig. 1c) as ompC is known to be up-regulated during high osmolarity conditions.<sup>32</sup> *Escherichia coli*  $\Delta ompC$  and *E. coli*  $\Delta ompC\text{-}\Delta ompF$  were both included as controls because ompF is known to be able to compensate for ompC function.<sup>33,34</sup> Modification of ompC in *E. coli* ompC\_gp61 did not affect its ability to survive under increased osmotic stress *in vitro* (Fig. 1c). Although deficiency of ompC alone had no effect in this *in vitro* assay, *E. coli* deficient in both ompC and ompF had reduced survival under high osmolarity conditions (Fig. 1c). We next tested the colonization capacity of these strains *in vivo*. *Escherichia coli* ompC\_gp61 colonized germ-free C57BL/6 mice to the same levels as wild-type *E. coli* (Fig. 1d). As a control in this *in vivo* assay, we found that only *E. coli*  $\Delta ompC\text{-}\Delta ompF$  displayed reduced colonization capacity. This demonstrated that the modified *E. coli* ompC\_gp61 strain had comparable fitness to the parent strain under *in vitro* and *in vivo* conditions.

### Immunogenicity of *E. coli* ompC\_gp61

We next tested whether the gp61 epitope within *E. coli* ompC\_gp61 was expressed and could be processed and presented to CD4<sup>+</sup> T cells by dendritic cells *in vitro*. Splenic C57BL/6 dendritic cells were incubated overnight with a fraction of enriched outer membrane proteins. Functional presentation was assessed by adding CFSE-labelled gp61-specific SMARTA T cells to the cultures the next day. *In vitro* proliferation by CFSE dilution was measured 5 days later (Fig. 2a). Only outer membrane proteins from *E. coli* ompC\_gp61 but not from wild-type *E. coli* or *E. coli*  $\Delta ompC$  resulted in the proliferation of gp61-specific SMARTA T cells (Fig. 2a), demonstrating the antigen specificity of the model. This also confirmed that

the mutation in the signal peptide (see Supplementary material, Fig. S1) did not affect trafficking of ompC\_gp61 to the outer membrane. Importantly, none of the protein fractions induced proliferation of polyclonal C57BL/6 T cells, further demonstrating an antigen-specific effect. As controls, antigen-specific stimulation with gp61 peptide alone induced proliferation of SMARTA T cells only while polyclonal stimulation with  $\alpha$ CD3 induced proliferation of both SMARTA and C57BL/6 T cells (Fig. 2a).

To test immunogenicity and antigen-specificity of the *E. coli* ompC\_gp61/SMARTA system *in vivo*,  $3 \times 10^7$  CFSE-labelled SMARTA T cells were transferred into wild-type C57BL/6 mice. One day later, mice were immunized intravenously with either  $10^8$  CFU *E. coli* ompC\_gp61 or wild-type *E. coli*. As a positive control, mice were injected with gp61 peptide in combination with the Toll-like receptor 9 ligand CpG. SMARTA T-cell proliferation in spleen and MLN was assessed by measuring CFSE dilution (Fig. 2b) and the proliferative index was calculated (Fig. 2c) 2 and 5 days later. As expected, wild-type *E. coli* did not induce proliferation of CFSE-labelled SMARTA T cells. In contrast, intravenous *E. coli* ompC\_gp61 specifically induced proliferation of SMARTA T cells. Interestingly, proliferation was restricted to the spleen and not observed in MLN. In contrast, control injections of gp61 peptide and CpG resulted in the proliferation of SMARTA T cells in both the spleen and MLN. Neither *E. coli* ompC\_gp61 nor wild-type *E. coli* induced proliferation of transferred CFSE-labelled ovalbumin-specific OT-II cells, further demonstrating the antigen specificity of the model (see Supplementary material, Fig. S2).

### Threshold for systemic antimicrobial CD4<sup>+</sup> T-cell responses

Since systemic reactivity against ompC can be measured in healthy humans,<sup>11</sup> we next determined the load of systemic bacteria that is required to trigger antigen-specific antimicrobial CD4<sup>+</sup> T cells in our model. We transferred  $3 \times 10^7$  CFSE-labelled CD4<sup>+</sup> SMARTA T cells into wild-type C57BL/6 mice and 1 day later a range of  $10^3\text{--}10^8$  CFU of *E. coli* ompC\_gp61 were given intravenously. As a negative control, a high dose of  $10^8$  CFU wild-type *E. coli* was administered. Proliferation of antigen-specific CD4<sup>+</sup> T cells was assessed 6 days later by CFSE dilution (Fig. 3a,b) and calculation of the proliferative index (Fig. 3c). We found that a relatively high dose of  $10^5\text{--}10^6$  CFU *E. coli* ompC\_gp61 was required for induction of an efficient proliferative *E. coli* (gp61)-specific T-cell response, which we defined as greater than three cell divisions (Fig. 3a). This threshold level is likely to be underestimated because of the high number of transferred SMARTA T cells and the possibility of bacterial *in vivo* proliferation.

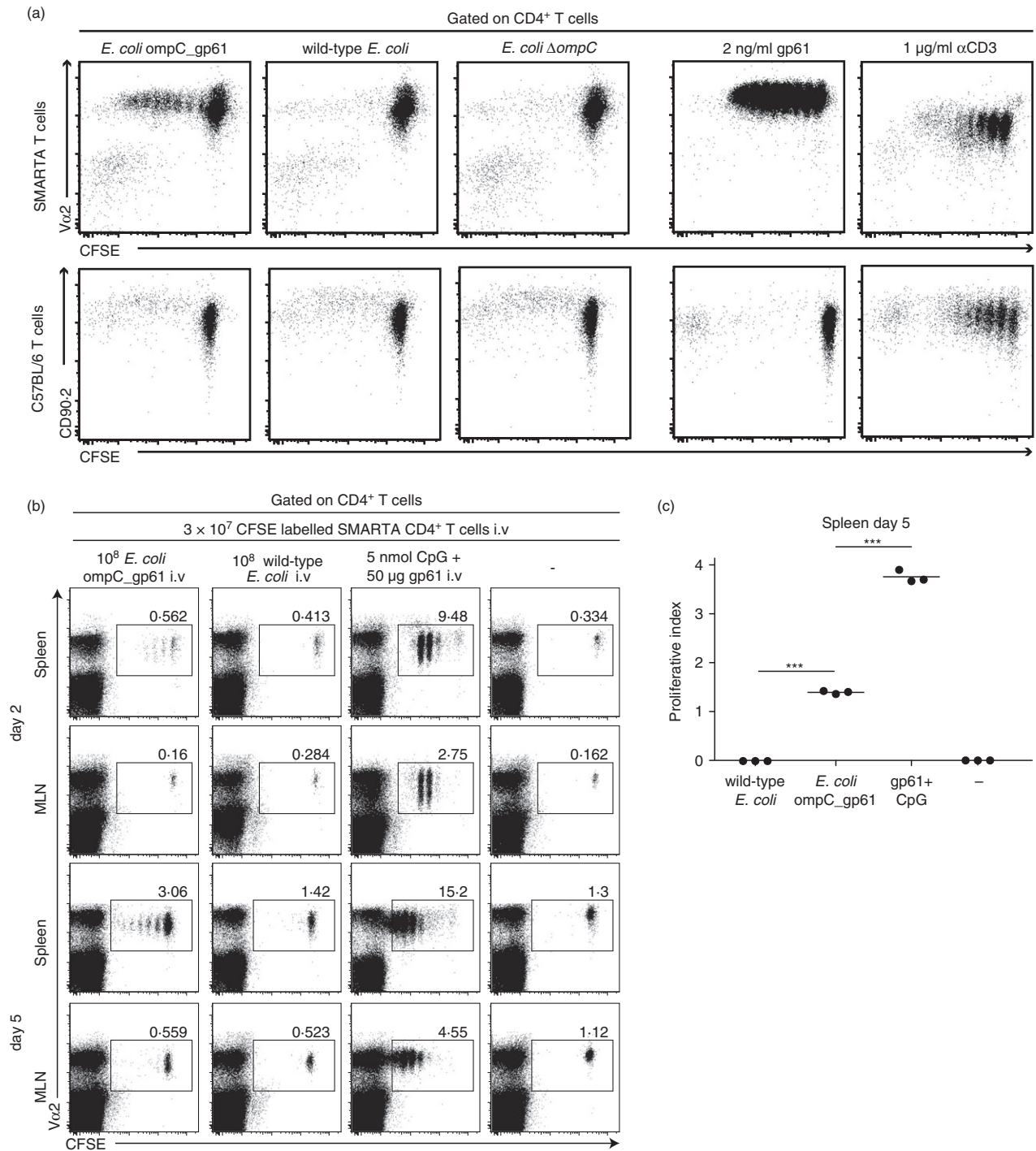


**Figure 2.** *In vivo* immunogenicity of live *Escherichia coli* ompC\_gp61. (a)  $5 \times 10^4$  splenic C57BL/6 dendritic cells (DC) were incubated overnight either with 5  $\mu$ g/ml outer membrane protein fractions from the indicated *E. coli* strains, 2 ng/ml gp61 peptide, or 1  $\mu$ g/ml  $\alpha$ CD3. The next day  $2 \times 10^5$  CFSE-labelled SMARTA or C57BL/6 CD4<sup>+</sup> T cells were added and proliferation was measured 5 days later by flow cytometry. (b)  $3 \times 10^7$  CFSE-labelled SMARTA T cells were adoptively transferred into C57BL/6 recipients (three mice per group). The next day  $10^8$  CFU wild-type *E. coli*,  $10^8$  CFU *E. coli* ompC\_gp61, or 5 nmol CpG + 50  $\mu$ g gp61 peptide were injected intravenously. SMARTA T-cell proliferation was measured in spleen and mesenteric lymph nodes (MLN) at day 2 and day 5 by flow cytometry. (c) Proliferative index of SMARTA T cells in the spleen at day 5. Data shown are representative of two or three independent experiments. \*\*\* $P < 0.0005$ .

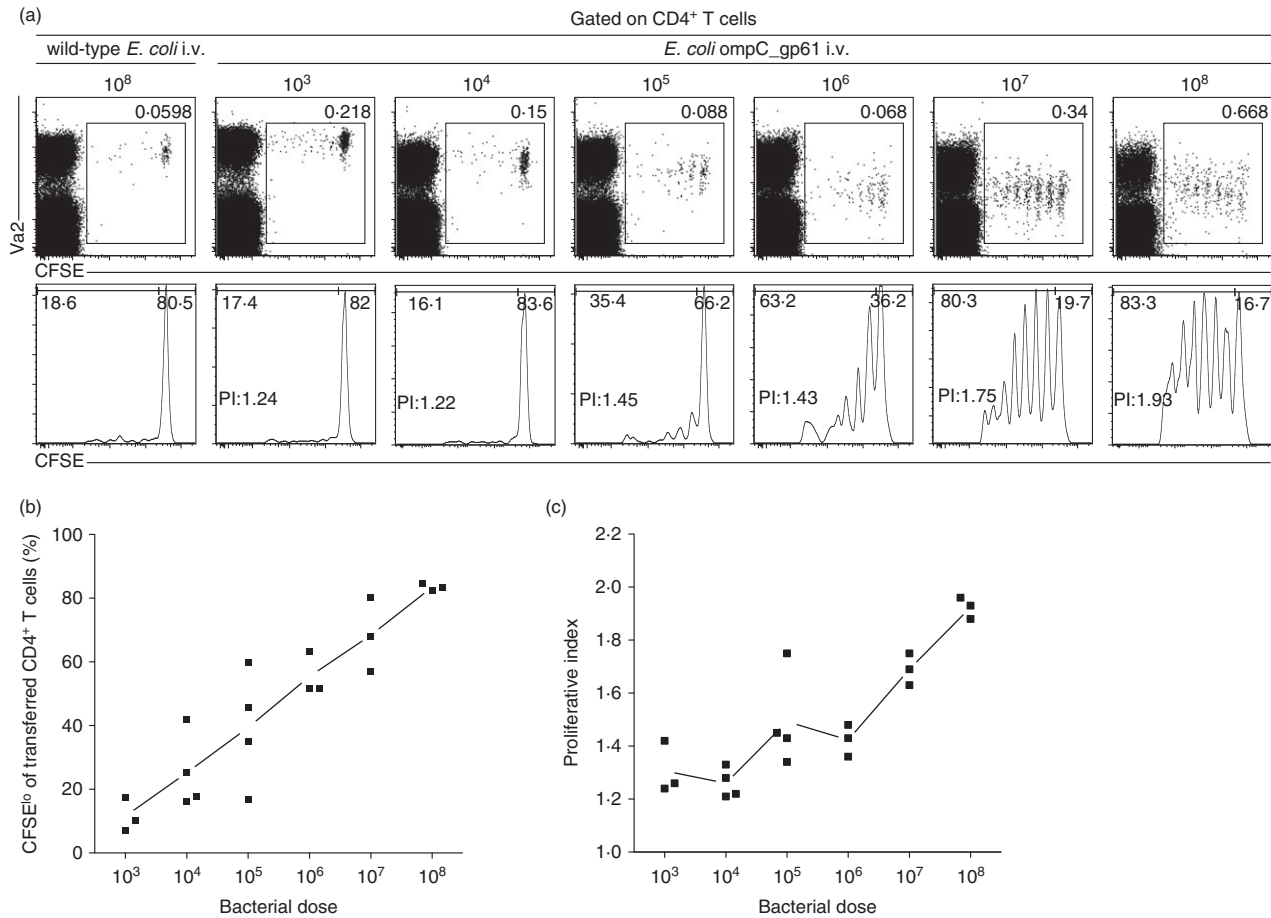


**Figure 3.** Threshold for induction of systemic antimicrobial CD4<sup>+</sup> T-cell responses. (a)  $3 \times 10^7$  CFSE-labelled SMARTA T cells were adoptively transferred into C57BL/6 recipients (three or four mice per group). The next day  $10^3$ – $10^8$  CFU *Escherichia coli* ompC\_gp61 or  $10^8$  CFU wild-type *E. coli* were injected intravenously. T-cell proliferation was measured at day 6 in the spleen. (b) Proportion of CFSE<sup>lo</sup> SMARTA T cells at day 6. (c) Proliferative index at day 6. Data shown are representative of two independent experiments.

### Impact of colonization status on threshold dose

It is known that the colonization status of the host can impact on systemic immunity.<sup>35–37</sup> In particular, germ-free mice that have an immature and underdeveloped immune system or mice treated with antibiotics have impaired innate and adaptive immune responses in models of viral and bacterial infections.<sup>35–37</sup> We therefore tested whether the colonization status of the recipient mouse could have an impact on the observed bacterial threshold for the induction of systemic CD4<sup>+</sup> T-cell proliferation. CFSE-labelled CD4<sup>+</sup> SMARTA T cells ( $3 \times 10^7$ ) were adoptively transferred into germ-free mice or gnotobiotic mice colonized with the ASF, a minimal flora consisting of eight bacterial species,<sup>23</sup> that has previously been demonstrated to normalize the intestinal immune system by inducing regulatory T cells.<sup>24</sup> One day after SMARTA T-cell transfer, the mice were systemically challenged with  $10^6$  or  $10^8$  CFU of *E. coli* ompC\_gp61. Six days later, *E. coli*-specific T-cell proliferation was measured by CFSE

dilution (Fig. 4a,b) and the proliferative index was calculated (Fig. 4c). Induction and magnitude of antigen-specific T-cell proliferation in the spleen was independent from the colonization status of the recipient (Fig. 4a). This was also reflected in the proportion of CFSE<sup>lo</sup> cells (Fig. 4b) and the proliferative index (Fig. 4c).

### Levels and kinetics of bacteraemia in the blood following intravenous *E. coli* application

We next examined the levels and kinetics of bacteraemia induced following intravenous injection of *E. coli* ompC\_gp61 to better understand the rather high threshold level of  $10^5$ – $10^6$  CFU and to ask what levels of bacteraemia the systemic immune system is exposed to over time. We determined the kinetics of bacterial clearance in the blood following intravenous injection of  $10^4$ ,  $10^6$  or  $10^8$  CFU *E. coli* ompC\_gp61 (Fig. 5a). Although  $10^4$  CFU are cleared from the peripheral blood to below detectable



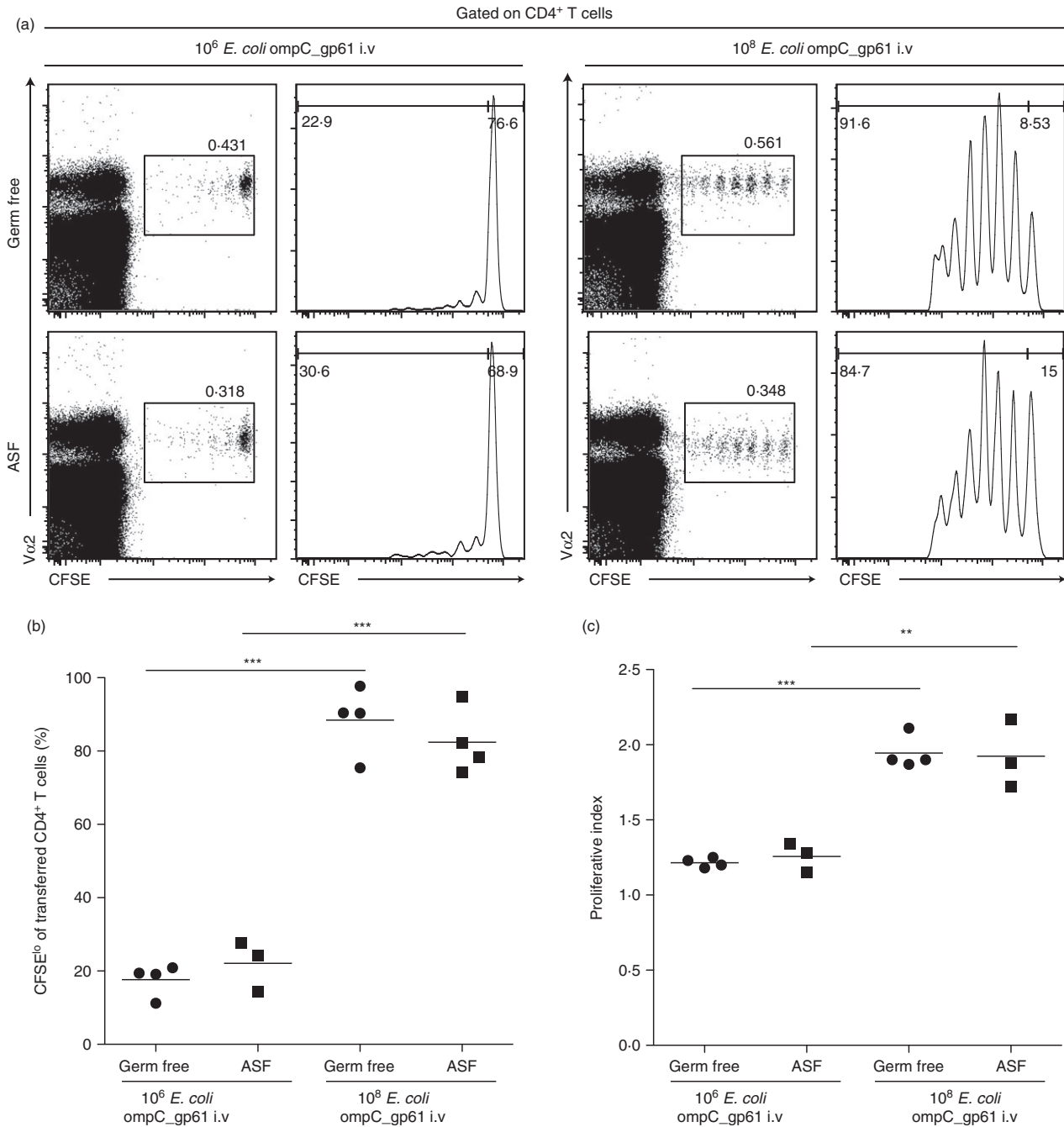


**Figure 4.** Impact of colonization status on systemic threshold. (a)  $3 \times 10^7$  CFSE-labelled SMARTA T cells were adoptively transferred into germ-free or altered Schaedler flora (ASF) colonized C57BL/6 recipients (three or four mice per group). The next day  $10^6$  or  $10^8$  CFU *Escherichia coli* ompC\_gp61 were injected intravenously. T-cell proliferation was measured at day 6 in the spleen. (b) Proportion of CFSE<sup>lo</sup> SMARTA T cells at day 6. (c) Proliferative index at day 6. \*\* $P < 0.005$ , \*\*\* $P < 0.0005$ .

levels in <1 hr, the threshold dose of  $10^6$  CFU caused a bacteraemia for 4–6 hr, and  $10^8$  CFU persisted for more than 12 hr (Fig. 5a). Most of these bacteria are probably cleared very quickly by the innate immune system, but some bacteria are trapped in the spleen and the liver and therefore were detectable in these organs up to 8 hr post-

challenge, even following a low dose of  $10^4$  CFU (Fig. 5b). Therefore, despite rapid clearance from the blood, bacteria can persist for longer time periods in the spleen or liver. Importantly, persistence of bacteria, particularly in the spleen, has the potential to induce strong adaptive responses.<sup>10</sup>

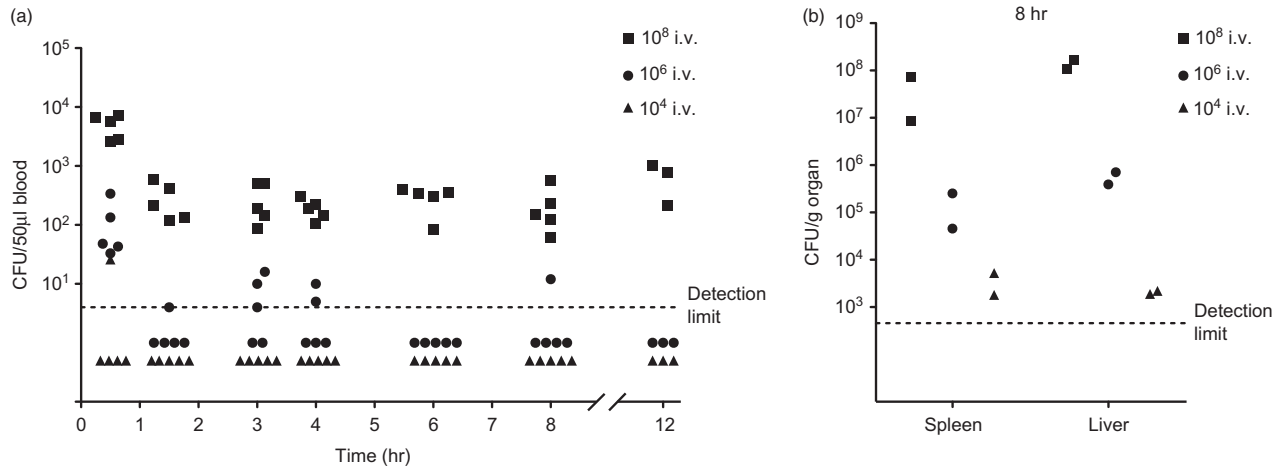


**Figure 5.** Systemic clearance of *Escherichia coli* ompC\_gp61. (a) Bacteraemia levels in the blood following intravenous injection of the indicated doses of *E. coli* ompC\_gp61 into C57BL/6 mice. (b) Bacterial loads in spleen and liver 8 hr following intravenous injection were measured by aerobic plating on Luria–Bertani plates. Combined data from two independent experiments are shown.

### Consequences of systemic antimicrobial CD4<sup>+</sup> T-cell reactivity following intestinal barrier disruption by DSS

We next investigated whether the threshold for systemic antimicrobial CD4<sup>+</sup> T-cell responses is altered following disruption of intestinal barrier function and epithelial permeability. To induce damage to the colon epithelium we treated wild-type gnotobiotic ASF-colonized C57BL/6 mice with 2% DSS in the drinking water. Importantly, gnotobiotic ASF C57BL/6 mice are not *E. coli* colonization resistant (Fig. 6a) and gnotobiotic ASF mice do not display lethality following DSS treatment, as observed for germ-free mice.<sup>38</sup> Furthermore, we have previously shown that DSS treatment of gnotobiotic ASF mice does not result in overt intestinal inflammation as observed in specific pathogen-free mice.<sup>24</sup> Therefore, DSS treatment of ASF mice predominantly affects barrier function and does not induce overt inflammation. This made it an ideal model to study subclinical bacterial translocation. CFSE-labelled SMARTA T cells were adoptively transferred into C57BL/6 recipients 2 days after initiation of DSS treatment and 1 day later mice were orally gavaged with 10<sup>10</sup> CFU of *E. coli* ompC\_gp61 or wild-type *E. coli*. Bacterial translocation was measured in MLN, liver and spleen 6 days later (Fig. 6b,c).

Both wild-type *E. coli* and *E. coli* ompC\_gp61 colonized ASF C57BL/6 mice to comparable levels in the presence or absence of DSS (Fig. 6a). *Escherichia coli* ompC\_gp61 reached slightly lower colonization levels compared with wild-type *E. coli* (not statistically significant) in gnotobiotic ASF mice in the absence of DSS. The *in vivo* colonization fitness of wild-type *E. coli* and *E. coli* ompC\_gp61 in germ-free mice was identical (Fig. 1d), but this might indicate that *E. coli* ompC\_gp61 has a

slightly reduced colonization fitness compared with wild-type *E. coli* in ASF mice where it has to compete against other bacteria. Nevertheless, in the presence of DSS treatment the colonization levels for wild-type *E. coli* and *E. coli* ompC\_gp61 were identical again. In the absence of DSS treatment very limited translocation of *E. coli* (wild-type and ompC\_gp61) to MLN (Fig. 6b), liver and spleen (Fig. 6c) was observed in the presence of transferred gp61-specific SMARTA T cells.

Treatment with DSS only marginally increased the level of translocation of wild-type *E. coli* and endogenous *Lactobacillus*. Translocation of other ASF species, such as *Bacteroides*, was not tested because translocation of these non-gp61-expressing ASF species is probably a bystander effect. The *Lactobacillus* ASF species is the only ASF species able to grow aerobically on LB plates, which is why it is reported here.

However, in the combined presence of gp61-specific CD4<sup>+</sup> T cells and *E. coli* ompC\_gp61 colonization, DSS treatment resulted in a dramatic increase of translocation of *E. coli* (and *Lactobacillus*) to MLN, liver and spleen (Fig. 6b,c). This effect was absolutely dependent on the presence of the gp61-specific SMARTA T cells because DSS treatment of ASF mice colonized with either wild-type *E. coli* or *E. coli* ompC\_gp61 in the absence of transferred SMARTA T cells (only endogenous C57BL/6 T cells present) did not induce bacterial translocation to liver or spleen (Fig. 6c). It is therefore not an intrinsic effect of the modified *E. coli* ompC\_gp61 strain. These data indicated that during DSS-induced epithelial damage, the transferred systemic *E. coli*-specific CD4<sup>+</sup> SMARTA T cells recognized the cognate gp61 epitope derived from *E. coli* ompC\_gp61, resulting in increased bacterial translocation.

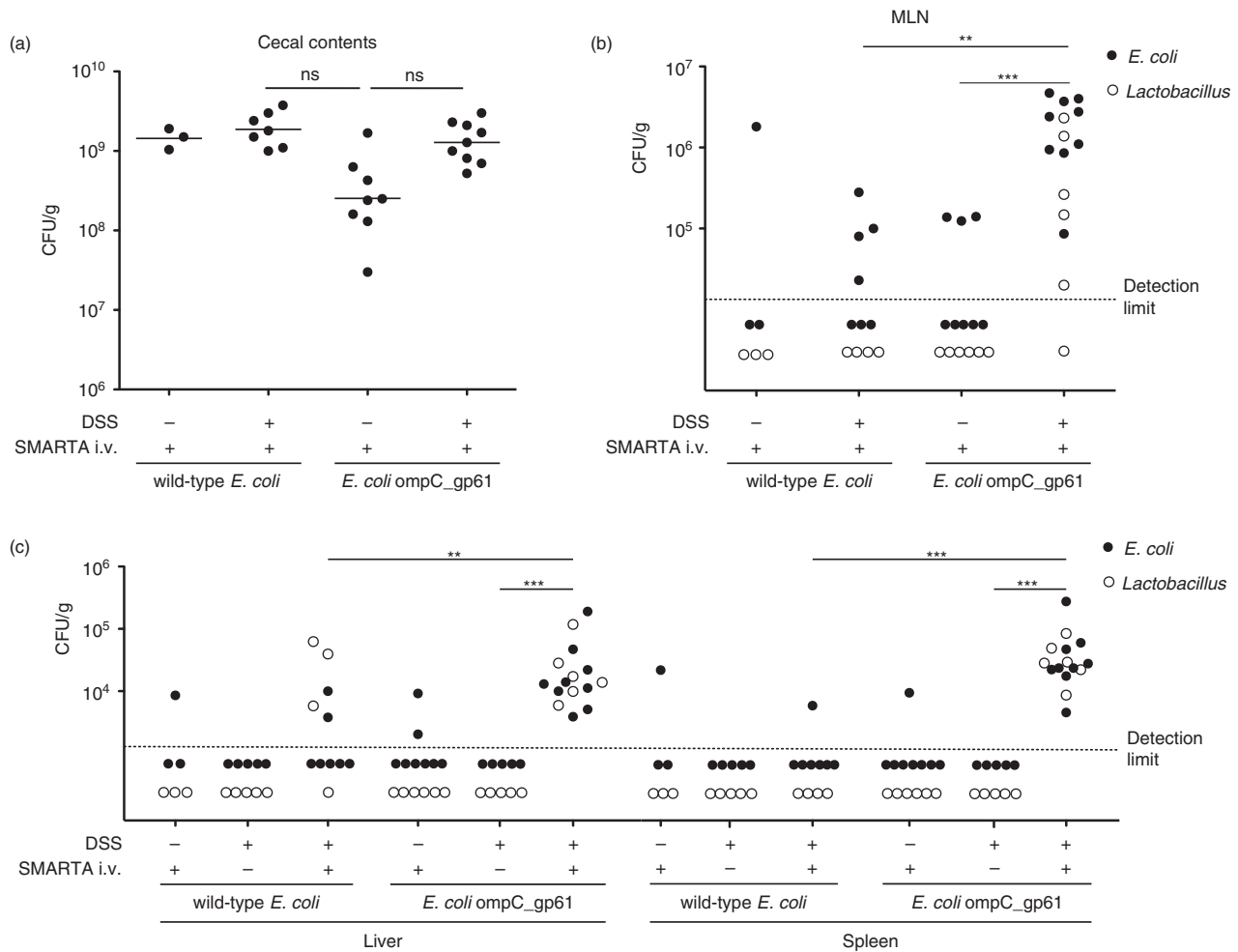


**Figure 6.** Bacterial translocation following dextran sodium sulphate (DSS) treatment. Altered Schaedler flora (ASF) colonized C57BL/6 mice were given 2% DSS in the drinking water or left untreated. On day 2,  $3 \times 10^7$  CFSE-labelled SMARTA T cells were adoptively transferred and the next day mice were gavaged with  $10^{10}$  CFU wild-type *Escherichia coli* or *E. coli* ompC\_gp61. All groups were analysed 6 days after bacterial challenge. (a) *Escherichia coli* colonization levels in caecal contents. (b and c) Translocation of *E. coli* and indigenous ASF *Lactobacillus* to the mesenteric lymph nodes (MLN) (b), liver and spleen (c) was measured by aerobic plating on Luria–Bertani plates. Combined data from three independent experiments are shown. ns = not significant, \*\* $P < 0.005$ , \*\*\* $P < 0.0005$  (using Mann–Whitney *U*-test).

We also measured intestinal permeability by assessing albumin concentrations in the caecal content. Whereas increased permeability was clearly increased in DSS-treated groups compared with non-DSS-treated, no significant differences between the wild-type *E. coli* and *E. coli* ompC\_gp61 groups were observed (see Supplementary material, Fig. S3). This suggests that increased bacterial numbers in liver and spleen might reflect increased bacterial proliferation, or that quantifying albumin in caecal content does not reflect the same mechanism of permeability that leads to the increased numbers of bacteria observed.

We next measured whether the transferred CFSE-labelled CD4<sup>+</sup> SMARTA T cells efficiently homed to the colon and whether they proliferated under these different conditions. Although the transferred SMARTA T cells were readily detectable in the spleen and MLN, we could not detect any signs of proliferation (Fig. 7a) or

activation as measured by surface activation markers (see Supplementary material, Fig. S4). This is probably because the levels of translocated *E. coli* ompC\_gp61 in the presence of DSS (Fig. 6c) did not reach the threshold required to induce proliferation. Only a very small population of *E. coli* (gp61)-specific SMARTA T cells could be detected in the colon lamina propria in all experimental groups (Fig. 7a). In addition, we could not detect any differences in the production of interferon- $\gamma$  or IL-17 by the transferred CFSE<sup>+</sup> SMARTA T cells or the endogenous CFSE<sup>-</sup> T-cell population between the different groups (Fig. 7b). This, surprisingly rather non-responsive T-cell phenotype was not caused by conversion of the transferred SMARTA T cells to a Foxp3<sup>+</sup> regulatory phenotype in the colon, MLN or spleen (see Supplementary material, Fig. S5). Furthermore, the difference in bacterial translocation following DSS treatment in the presence of

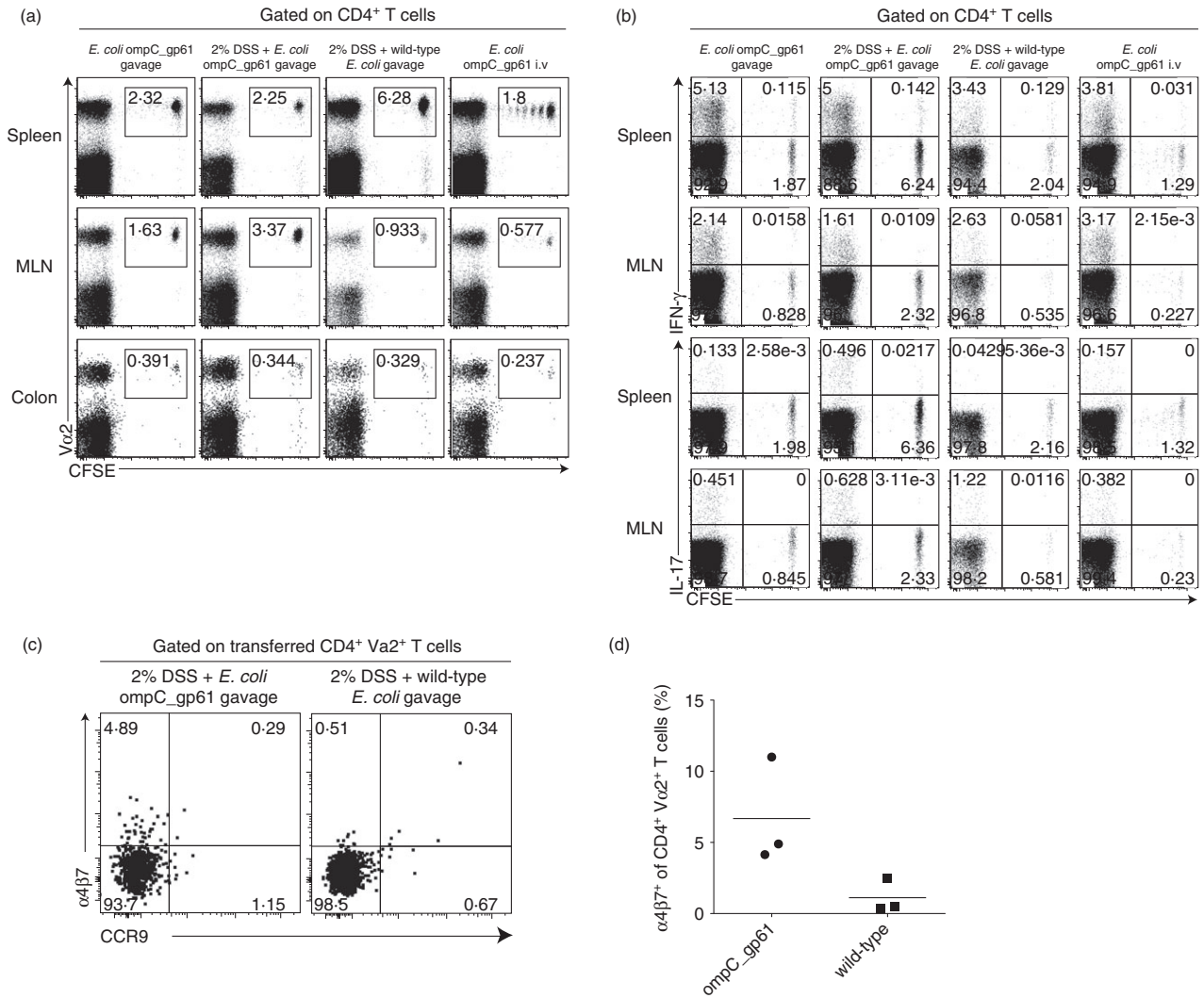


**Figure 7.** Absence of SMARTA T-cell proliferation following dextran sodium sulphate (DSS) treatment. (a) Altered Schaedler flora (ASF) colonized C57BL/6 mice were given 2% DSS in the drinking water or left untreated. On day 2,  $3 \times 10^7$  CFSE-labelled SMARTA T cells were adoptively transferred and the next day mice were gavaged with  $10^{10}$  CFU wild-type *Escherichia coli* or *E. coli* ompC\_gp61. As positive control for proliferation, untreated C57BL/6 mice that received  $3 \times 10^7$  CFSE-labelled SMARTA T cells were intravenously injected with *E. coli* ompC\_gp61. All groups were analysed 6 days after bacterial challenge. (a) Proliferation of CFSE-labelled SMARTA T cells in spleen, mesenteric lymph node (MLN), and colon was measured by flow cytometry. (b) Cytokine production in spleen and MLN was measured by intracellular cytokine staining following stimulation with PMA and Ionomycin. (c, d) Expression of intestinal homing markers  $\alpha_4\beta_7$  and CCR9 on splenic SMARTA T cells was measured by flow cytometry.

*E. coli* ompC\_gp61 or wild-type *E. coli* was not caused by differential activation of the intestinal innate immune system or by changes in the inflammatory status between the groups, as determined by measuring cytokine levels in the serum (see Supplementary material, Fig. S6). Although there was a trend towards increased levels of IL-6 in the DSS-treated groups colonized with *E. coli* ompC\_gp61, this did not reach statistical significance (see Supplementary material, Fig. S6).

The lack of efficient homing of the transferred SMARTA T cells to the colon lamina propria (Fig. 7a) could be due to the intestinal niche being completely occupied by the endogenous C57BL/6 T-cell population.

We therefore repeated the same experimental set up in T-cell (and B-cell) -deficient ASF RAG-1<sup>-/-</sup> recipients with no endogenous T-cell compartment. Although we observed a higher proportion of  $\alpha_4\beta_7^+$  SMARTA T cells in the spleen of DSS treated RAG-1<sup>-/-</sup> mice colonized with *E. coli* ompC\_gp61 compared with wild-type *E. coli* (Fig. 7c,d), we again did not observe efficient homing of Va2<sup>+</sup> T cells to the colon lamina propria even in the absence of endogenous T cells (see Supplementary material, Fig. S5). This indicated that DSS treatment of gnotobiotic ASF mice does not result in sufficient intestinal inflammatory signals to efficiently attract antigen-specific T cells.

We therefore conclude that the presence of systemic *E. coli* (gp61)-specific antimicrobial SMARTA T cells has a detrimental impact on mucosal integrity under certain conditions. It remains unclear how exactly the SMARTA T cells exert this effect at the mucosa. It is therefore important to further dissect the detrimental versus beneficial consequences of systemic antimicrobial T-cell reactivity for mucosal homeostasis.

## Discussion

Immune compartmentalization of the mucosal and systemic immune system is critical for the maintenance of host–microbe mutualism<sup>5,7,8</sup> and its breakdown can result in systemic antimicrobial immune reactivity.<sup>5,7</sup> Innate immune function is crucial to control microbes that translocate into the mucosal tissues and hence innate immune deficiency results in the induction of systemic antimicrobial antibodies to control systemic bacteraemia.<sup>9</sup> In addition, mutations in innate immunity genes are often associated with autoinflammatory diseases including IBD.<sup>39–41</sup> The role of systemic antimicrobial CD4<sup>+</sup> T-cell reactivity in host–microbe mutualism, however, remains less clear.

Antimicrobial T-cell responses have previously been characterized for example using T-cell receptor transgenic CBir1 mice.<sup>31</sup> This model allows the measurement of immune responses against flagellated bacteria expressing the flagellin antigen CBir1. As flagellin is expressed by a wide range of bacterial species, the CBir1 model does not allow a precise study of antigen-specific antimicrobial reactivity against a single bacterial species (or even a single species-specific epitope). Furthermore, even using gnotobiotic technology, it is impossible to generate identical microbiotas where the only difference is the lack or presence of the flagellin epitope for experimental purposes. Therefore, to measure antigen-specific antimicrobial CD4<sup>+</sup> T-cell responses in precisely defined experimental settings, we deliberately generated a novel model to study species-specific antimicrobial T-cell responses. We generated a genetically modified *E. coli* ompC\_gp61 strain that expresses the lymphocytic choriomeningitis virus-derived T helper cell epitope gp61, allowing the measurement of specific antimicrobial T-cell responses against a defined antigen. The gp61 epitope was inserted into loop 7 of ompC because systemic immune reactivity against ompC has previously been observed in IBD patients,<sup>42</sup> making this a clinically relevant antigen in the context of IBD. The inserted gp61 is therefore a true bacterial neo-antigen and it is irrelevant that it was originally identified in a virus.

Using this new model, we found that the threshold for induction of proliferation of systemic antimicrobial T-cell proliferation was very high. The threshold for

proliferation was so high that it could not even be reached following DSS treatment to induce damage to the colon epithelium. This high threshold for proliferation is probably due to rapid clearance of systemic bacteria by the innate immune system. In addition, high enough numbers of live bacteria need to be trapped in the spleen, for example in marginal zone macrophages,<sup>18</sup> for long enough to induce an adaptive antimicrobial T-cell response. This is in line with the notion that the systemic immune system is not tolerant to the presence of gut-derived bacteria<sup>6</sup> and has evolved to respond to only the persistent presence of a high dose of bacteria.

Although bacterial translocation induced by DSS treatment did not induce antimicrobial T-cell proliferation, the presence of antimicrobial CD4<sup>+</sup> T helper cells during DSS treatment had a detrimental effect on bacterial translocation by dramatically increasing the number of bacteria that translocated to the spleen or liver. This effect was strictly dependent on the presence of the transferred SMARTA T cells. This is therefore a clear indication that systemic antimicrobial T-cell (hyper-)reactivity can have detrimental consequences for host–microbe mutualism. Interestingly, this is in contrast to systemic antimicrobial antibody responses that have been shown to be beneficial in the face of systemic bacteraemia due to innate immune deficiency.<sup>9</sup> This suggests that systemic antimicrobial antibody and T-cell responses might be regulated differently and that different immune mechanisms are in place to ensure host–microbe mutualism.

The exact mechanism by which the presence of microbe-specific CD4<sup>+</sup> T cells mediated increased bacterial translocation remains unclear as we could, surprisingly, detect very few interferon- $\gamma$ -, IL-17- or IL-10-producing SMARTA T cells in the colonic lamina propria. Although it is known that regulatory T-cell conversion to an oral antigen occurs in the MLN at around day 5 followed by migration to the colon and subsequent regulatory T-cell proliferation in the colon,<sup>43</sup> we could not detect any regulatory T-cell conversion in colon or MLN in our experimental model (see Supplementary material, Fig. S5). However, transferred SMARTA T cells in the spleen expressed gut homing markers  $\alpha_4\beta_7$  following priming with gp61 neo-antigen, which suggested that increased homing of antigen-specific T cells to the intestine could be one of the mechanisms that are responsible for negatively regulating the gut epithelial integrity and thereby promoting systemic bacterial translocation. How exactly these T cells mediate this effect locally needs to be further investigated. For example, other pro-inflammatory cytokines including tumour necrosis factor- $\alpha$ , IL-6 or interferon- $\gamma$  have been shown to promote apoptosis of epithelial cells or modulate the expression of claudins, which are tight junction proteins required for the regulation of intestinal permeability.<sup>44–47</sup> Importantly, increased intestinal permeability has been involved in the



pathogenesis of IBD<sup>48</sup> and clinical studies have shown that there is a decrease in the expression of tight junction proteins in IBD patients.<sup>49</sup> Although it is also possible that activation of systemic anti-microbial CD4<sup>+</sup> T cells could impact on the function of innate lymphoid cells that have been shown to be involved in anatomical containment of commensal bacteria,<sup>50</sup> we found no differences in the innate compartment, in line with the notion that the observed increased systemic bacterial translocation following DSS-induced gut epithelial damage is antigen-specific T-cell driven. This demonstrates that systemic antimicrobial T cells may have pathogenic consequences under certain conditions.

Taken together, we demonstrate here that systemic antimicrobial T-cell (hyper-)reactivity can have a detrimental effect on host–microbe mutualism. Elucidating the mechanisms by which systemic antimicrobial T cells promote systemic bacterial translocation could therefore provide insights into the possible role of systemic antimicrobial CD4<sup>+</sup> T cells in the pathogenesis of IBD.

## Acknowledgements

MBG was supported by the AbbVie IBD grant 2015 and an Ambizione fellowship from the Swiss National Science Foundation (SNSF). FR was supported by a Marie Heim-Vögtlin fellowship from the SNSF. We thank Prof. Kathy McCoy and Prof. Andrew Macpherson for their support and critical reading of the manuscript. We also thank the Clean Mouse Facility (CMF) of the University of Bern for germ-free and gnotobiotic mouse husbandry.

## Disclosures

The authors declare that they do not have a conflict of interest.

## References

- Sartor RB. Microbial influences in inflammatory bowel diseases. *Gastroenterology* 2008; **134**:577–94.
- Albert MJ, Mathan VI, Baker SJ. Vitamin B12 synthesis by human small intestinal bacteria. *Nature* 1980; **283**:781–2.
- Treparoli V, Backhed F. Functional interactions between the gut microbiota and host metabolism. *Nature* 2012; **489**:242–9.
- Geuking MB, Koller Y, Rupp S, McCoy KD. The interplay between the gut microbiota and the immune system. *Gut Microbes* 2014; **5**:411–8.
- Macpherson AJ, Gatto D, Sainsbury E, Harriman GR, Hengartner H, Zinkernagel RM. A primitive T cell-independent mechanism of intestinal mucosal IgA responses to commensal bacteria. *Science* 2000; **288**:2222–6.
- Macpherson AJ, Uhr T. Induction of protective IgA by intestinal dendritic cells carrying commensal bacteria. *Science* 2004; **303**:1662–5.
- Macpherson AJ, Uhr T. Compartmentalization of the mucosal immune responses to commensal intestinal bacteria. *Ann N Y Acad Sci* 2004; **1029**:36–43.
- Konrad A, Cong Y, Duck W, Borlaza R, Elson CO. Tight mucosal compartmentation of the murine immune response to antigens of the enteric microbiota. *Gastroenterology* 2006; **130**:2050–9.
- Slack E, Hapfelmeier S, Stecher B, Velykoredko Y, Stoel M, Lawson MA *et al.* Innate and adaptive immunity cooperate flexibly to maintain host–microbiota mutualism. *Science* 2009; **325**:617–20.
- Medzhitov R. Recognition of microorganisms and activation of the immune response. *Nature* 2007; **449**:819–26.
- Mei L, Targan SR, Landers CJ, Dutridge D, Ippoliti A, Vasilias EA *et al.* Familial expression of anti-*Escherichia coli* outer membrane porin C in relatives of patients with Crohn's disease. *Gastroenterology* 2006; **130**:1078–85.
- Guttman JA, Finlay BB. Tight junctions as targets of infectious agents. *Biochim Biophys Acta* 2009; **1788**:832–41.
- Lucas VS, Gafan G, Dewhurst S, Roberts GJ. Prevalence, intensity and nature of bacteraemia after toothbrushing. *J Dent* 2008; **36**:481–7.
- Sighthorsson G, Simpson RJ, Walley M, Anthony A, Foster R, Hotz-Behofitsitz C *et al.* COX-1 and 2, intestinal integrity, and pathogenesis of nonsteroidal anti-inflammatory drug enteropathy in mice. *Gastroenterology* 2002; **122**:1913–23.
- Stenman LK, Holma R, Eggert A, Korpela R. A novel mechanism for gut barrier dysfunction by dietary fat: epithelial disruption by hydrophobic bile acids. *Am J Physiol Gastrointest Liver Physiol* 2013; **304**:G227–34.
- Stenman LK, Holma R, Korpela R. High-fat-induced intestinal permeability dysfunction associated with altered fecal bile acids. *World J Gastroenterol* 2012; **18**:923–9.
- Hand TW, Dos Santos LM, Boudadoux N, Molloy MJ, Pagan AJ, Pepper M *et al.* Acute gastrointestinal infection induces long-lived microbiota-specific T cell responses. *Science* 2012; **337**:1553–6.
- Aichele P, Zinke J, Grode L, Schwendener RA, Kaufmann SH, Seiler P. Macrophages of the splenic marginal zone are essential for trapping of blood-borne particulate antigen but dispensable for induction of specific T cell responses. *J Immunol* 2003; **171**:1148–55.
- Conlan JW. Critical roles of neutrophils in host defense against experimental systemic infections of mice by *Listeria monocytogenes*, *Salmonella typhimurium*, and *Yersinia enterocolitica*. *Infect Immun* 1997; **65**:630–5.
- Hirakata Y, Kaku M, Furuya N, Matsumoto T, Tateda K, Tomono K *et al.* Effect of clearance of bacteria from the blood on the development of systemic bacteraemia in mice. *J Med Microbiol* 1993; **38**:337–44.
- McDonald B, Urrutia R, Yipp BG, Jenne CN, Kubes P. Intravascular neutrophil extracellular traps capture bacteria from the bloodstream during sepsis. *Cell Host Microbe* 2012; **12**:324–33.
- Actis GC, Rosina F, Mackay IR. Inflammatory bowel disease: beyond the boundaries of the bowel. *Expert Rev Gastroenterol Hepatol* 2011; **5**:401–10.
- Dewhurst FE, Chien CC, Paster BJ, Ericson RL, Orcutt RP, Schauer DB *et al.* Phylogeny of the defined murine microbiota: altered Schaedler flora. *Appl Environ Microbiol* 1999; **65**:3287–92.
- Geuking MB, Cahenzli J, Lawson MA, Ng DC, Slack E, Hapfelmeier S *et al.* Intestinal bacterial colonization induces mutualistic regulatory T cell responses. *Immunity* 2011; **34**:794–806.
- Stecher B, Chaffron S, Kappeli R, Hapfelmeier S, Freedrich S, Weber TC *et al.* Like will to like: abundances of closely related species can predict susceptibility to intestinal colonization by pathogenic and commensal bacteria. *PLoS Pathog* 2010; **6**:e1000711.
- Karlinsky JE.  $\lambda$ -Red genetic engineering in *Salmonella enterica* serovar Typhimurium. *Methods Enzymol* 2007; **421**:199–209.
- Maloy SR, Nunn WD. Selection for loss of tetracycline resistance by *Escherichia coli*. *J Bacteriol* 1981; **145**:1110–1.
- Ghosh R, Steiert M, Hardmeyer A, Wang YF, Rosenbusch JP. Overexpression of outer membrane porins in *E. coli* using pBluescript-derived vectors. *Gene Expr* 1998; **7**:149–61.
- Oxenius A, Bachmann MF, Zinkernagel RM, Hengartner H. Virus-specific MHC-class II-restricted TCR-transgenic mice: effects on humoral and cellular immune responses after viral infection. *Eur J Immunol* 1998; **28**:390–400.
- Lee SY, Choi JH, Xu Z. Microbial cell-surface display. *Trends Biotechnol* 2003; **21**:45–52.
- Cong Y, Feng T, Fujihashi K, Schoeb TR, Elson CO. A dominant, coordinated T regulatory cell-IgA response to the intestinal microbiota. *Proc Natl Acad Sci USA* 2009; **106**:19256–61.
- Forst S, Delgado J, Ramakrishnan G, Inouye M. Regulation of ompC and ompF expression in *Escherichia coli* in the absence of envZ. *J Bacteriol* 1988; **170**:5080–5.
- Alphen WV, Lugtenberg B. Influence of osmolarity of the growth medium on the outer membrane protein pattern of *Escherichia coli*. *J Bacteriol* 1977; **131**:623–30.
- Misra R, Reeves PR. Role of micF in the tolC-mediated regulation of OmpF, a major outer membrane protein of *Escherichia coli* K-12. *J Bacteriol* 1987; **169**:4722–30.
- Abt MC, Osborne LC, Monticelli LA, Doering TA, Alenghat T, Sonnenberg GF *et al.* Commensal bacteria calibrate the activation threshold of innate antiviral immunity. *Immunity* 2012; **37**:158–70.
- Clarke TB, Davis KM, Lysenko ES, Zhou AY, Yu Y, Weiser JN. Recognition of peptidoglycan from the microbiota by Nod1 enhances systemic innate immunity. *Nat Med* 2010; **16**:228–31.
- Ganal SC, Sanos SL, Kalfass C, Oberle K, Johner C, Kirschning C *et al.* Priming of natural killer cells by nonmucosal mononuclear phagocytes requires instructive signals from commensal microbiota. *Immunity* 2012; **37**:171–86.

- 38 Maslowski KM, Vieira AT, Ng A, Kranich J, Sierro F, Yu D *et al.* Regulation of inflammatory responses by gut microbiota and chemoattractant receptor GPR43. *Nature* 2009; **461**:1282–6.
- 39 Hampe J, Cuthbert A, Croucher PJ, Mirza MM, Mascheretti S, Fisher S *et al.* Association between insertion mutation in NOD2 gene and Crohn's disease in German and British populations. *Lancet* 2001; **357**:1925–8.
- 40 Ogura Y, Bonen DK, Inohara N, Nicolae DL, Chen FF, Ramos R *et al.* A frameshift mutation in NOD2 associated with susceptibility to Crohn's disease. *Nature* 2001; **411**:603–6.
- 41 Hugot JP, Chamaillard M, Zouali H, Lesage S, Cezard JP, Belaiche J *et al.* Association of NOD2 leucine-rich repeat variants with susceptibility to Crohn's disease. *Nature* 2001; **411**:599–603.
- 42 Landers CJ, Cohavy O, Misra R, Yang H, Lin YC, Braun J *et al.* Selected loss of tolerance evidenced by Crohn's disease-associated immune responses to auto- and microbial antigens. *Gastroenterology* 2002; **123**:689–99.
- 43 Hadis U, Wahl B, Schulz O, Hardtke-Wolenski M, Schippers A, Wagner N *et al.* Intestinal tolerance requires gut homing and expansion of FoxP3<sup>+</sup> regulatory T cells in the lamina propria. *Immunity* 2011; **34**:237–46.
- 44 Bruewer M, Luegering A, Kucharzik T, Parkos CA, Madara JL, Hopkins AM *et al.* Proinflammatory cytokines disrupt epithelial barrier function by apoptosis-independent mechanisms. *J Immunol* 2003; **171**:6164–72.
- 45 Bruewer M, Utech M, Ivanov AI, Hopkins AM, Parkos CA, Nusrat A. Interferon- $\gamma$  induces internalization of epithelial tight junction proteins via a macropinocytosis-like process. *FASEB J* 2005; **19**:923–33.
- 46 Ma TY, Boivin MA, Ye D, Pedram A, Said HM. Mechanism of TNF- $\alpha$  modulation of Caco-2 intestinal epithelial tight junction barrier: role of myosin light-chain kinase protein expression. *Am J Physiol Gastrointest Liver Physiol* 2005; **288**:G422–30.
- 47 Schulzke JD, Bojarski C, Zeissig S, Heller F, Gitter AH, Fromm M. Disrupted barrier function through epithelial cell apoptosis. *Ann N Y Acad Sci* 2006; **1072**:288–99.
- 48 Welcker K, Martin A, Kolle P, Siebeck M, Gross M. Increased intestinal permeability in patients with inflammatory bowel disease. *Eur J Med Res* 2004; **9**:456–60.
- 49 Zeissig S, Burgel N, Gunzel D, Richter J, Mankertz J, Wahnschaffe U *et al.* Changes in expression and distribution of claudin 2, 5 and 8 lead to discontinuous tight junctions and barrier dysfunction in active Crohn's disease. *Gut* 2007; **56**:61–72.
- 50 Sonnenberg GF, Monticelli LA, Alenghat T, Fung TC, Hutnick NA, Kunisawa J *et al.* Innate lymphoid cells promote anatomical containment of lymphoid-resident commensal bacteria. *Science* 2012; **336**:1321–5.

## Supporting Information

Additional Supporting Information may be found in the online version of this article:

**Figure S1.** Schematic of the *Escherichia coli* ompC\_gp61 signal peptide. A schematic of the ompC\_gp61 construct is shown.

**Figure S2.** *In vivo* antigen-specificity control using ovalbumin (OVA) -specific CD4<sup>+</sup> OT-II T cells.  $3 \times 10^7$  CFSE-labelled CD4<sup>+</sup> OT-II T cells were adoptively transferred into C57BL/6 recipients. The next day  $10^8$  CFU of *Escherichia coli* ompC\_gp61 or wild-type *E. coli* were injected intravenously. As a positive control 50  $\mu$ g of OVA in combination with 5 nmol CpG were injected intravenously. 5 days later OT-II T cell proliferation was measured by flow cytometry. Data shown are representative of two independent experiments.

**Figure S3.** Intestinal permeability. Altered Schaedler flora (ASF) colonized C57BL/6 mice were given 2% dextran sodium sulphate in the drinking water or left untreated. On day 2,  $3 \times 10^7$  CFSE-labelled SMARTA T cells were adoptively transferred and the next day mice were gavaged with  $10^{10}$  CFU wild-type *Escherichia coli* or

*E. coli* ompC\_gp61. Albumin levels in the caecal content were measured 6 days after bacterial challenge in the different experimental groups. Values shown are mean  $\pm$  SD from three to four mice/group.

**Figure S4.** T-cell activation markers. Altered Schaedler flora (ASF) colonized C57BL/6 mice were given 2% dextran sodium sulphate in the drinking water or left untreated. On day 2,  $3 \times 10^7$  CFSE-labelled SMARTA T cells were adoptively transferred and the next day mice were gavaged with  $10^{10}$  CFU wild-type *Escherichia coli* or *E. coli* ompC\_gp61. The indicated activation markers were analysed by flow cytometry 6 days after bacterial challenge in colon, mesenteric lymph nodes (MLN) and spleen. Data represents mean  $\pm$  SD from three to four mice/group. \* $P < 0.05$ , \*\* $P < 0.005$ .

**Figure S5.** Absence of regulatory T (Treg) cell conversion. (a) Altered Schaedler flora (ASF) colonized C57BL/6 mice were given 2% dextran sodium sulphate (DSS) in the drinking water or left untreated. On day 2,  $3 \times 10^7$  CFSE-labelled SMARTA T cells were adoptively transferred and the next day mice were gavaged with  $10^{10}$  CFU wild-type *Escherichia coli* or *E. coli* ompC\_gp61. Treg cell conversion in colon, mesenteric lymph nodes (MLN) and spleen was analysed by flow cytometry 6 days after bacterial challenge. Representative dot plots from three to four mice/group are shown. (b) ASF RAG-1<sup>-/-</sup> mice were gavaged with  $10^{10}$  CFU wild-type *E. coli* or *E. coli* ompC\_gp61. On day 1, mice were given 2% DSS in the drinking water and also received  $1 \times 10^6$  SMARTA T cells intravenously on the same day. Homing to the colon was analysed 12 days after bacterial challenge by flow cytometry.

**Figure S6.** No changes in the intestinal innate immune system and inflammatory status. Altered Schaedler flora (ASF) colonized C57BL/6 mice were given 2% dextran sodium sulphate (DSS) in the drinking water. On day 2,  $3 \times 10^7$  CFSE-labelled SMARTA T cells were adoptively transferred and the next day mice were gavaged with  $10^{10}$  CFU wild-type *Escherichia coli* or *E. coli* ompC\_gp61. (a–e) All groups were analysed by flow cytometry 6 days after bacterial challenge. (a) Representative dot plots showing lineage negative (CD19<sup>-</sup> CD3<sup>-</sup>) cells and (b) MHC class II I-A<sup>b</sup> positive cells in the small intestine lamina propria. Proportions of (c) CD11b<sup>+</sup> CD11c<sup>-</sup>, (d) CD11b<sup>+</sup> CD11c<sup>+</sup> and (e) CD11b<sup>-</sup> CD11c<sup>+</sup> in the small intestine lamina propria are shown. Data represent pooled data from two independent experiments with three or four mice/group. (f) Serum levels of the indicated cytokines were measured. Data shown are from three pooled independent experiments. The horizontal line represents the geometric mean. The detection limit (DL) of the assay is indicated by a dotted horizontal line.